Bonded Exciplex Formation: Electronic and Stereoelectronic Effects†

Yingsheng Wang,‡ Olesya Haze,‡ Joseph P. Dinnocenzo,*,‡ Samir Farid,*,‡ Ramy S. Farid,*,§ and Ian R. Gould*,||

Department of Chemistry and Center for Photoinduced Charge Transfer, University of Rochester, Rochester, New York 14627, Schrödinger, Inc., 120 West 45th Street, 29th Floor, New York, New York 10036, and Department of Chemistry and Biochemistry, Arizona State University, Tempe, Arizona 85287

Received: May 10, 2008; Revised Manuscript Received: September 15, 2008

As recently proposed, the singlet-excited states of several cyanoaromatics react with pyridine via bonded-exciplex formation, a novel concept in photochemical charge transfer reactions. Presented here are electronic and steric effects on the quenching rate constants, which provide valuable support for the model. Additionally, excited-state quenching in poly(vinylpyridine) is strongly inhibited both relative to that in neat pyridine and also to conventional exciplex formation in polymers, consistent with a restrictive orientational requirement for the formation of bonded exciplexes. Examples of competing reactions to form both conventional and bonded exciplexes are presented, which illustrate the delicate balance between these two processes when their reaction energetics are similar. Experimental and computational evidence is provided for the formation of a bonded exciplex in the reaction of the singlet excited state of 2,6,9,10-tetracyanoanthracene (TCA) with an oxygen-substituted donor, dioxane, thus expanding the scope of bonded exciplexes.

Introduction

The quenching reactions of several excited-state electron acceptors by pyridine have recently been proposed to proceed through a new excited-state intermediate, a bonded exciplex.[1] The relationship between the electronic structure of a conventional exciplex and a bonded exciplex formed from reaction between an excited-state electron acceptor (A*) and an electron donor can be understood in terms of their principal, contributing valence bond configurations. The wave function for a conventional exciplex is generally described by eq 1, where the three contributing configurations are the radical ion pair ($A^{\bullet-}D^{\bullet+}$), the locally excited (LE) configuration (A*D), and the ground configuration (AD).[2,3] The wave function for the bonded exciplex, eq 2, differs from a conventional exciplex in that a bonded, charge-transfer configuration ($A^{-}-D^{+}$) replaces the radical−ion pair configuration. In cases where bonded exciplexes are formed, the energy of the bonded configuration is significantly lower than that of the radical−ion pair as a result of this bonding interaction.

$$\Psi(\mathrm{Ex}) = c_1\Psi(A^{\bullet-}D^{\bullet+}) + c_2\Psi(A^{*}D) + c_3\Psi(AD) \quad (1)$$

$$\Psi(\text{b-Ex}) = c_1'\Psi(A^{-}-D^{+}) + c_2'\Psi(A^{*}D) + c_3'\Psi(AD) \quad (2)$$

In the formation of conventional exciplexes, when the energy of the ($A^{\bullet-}D^{\bullet+}$) configuration exceeds that of the LE state by ~0.3 eV, the A* + D quenching reaction is usually too endothermic to compete with rapid decay of the excited state.[4] In contrast to this behavior, pyridine quenches the fluorescence of 9,10-dicyanoanthracene (DCA) with a rate constant that approaches the diffusion-controlled limit, even though formation of a radical−ion pair is endothermic by ~0.6 eV. A conventional exciplex is energetically inaccessible in this case, and formation of a bonded exciplex has been proposed.[1] The rapid quenching of DCA* by pyridine via bonded exciplex formation can be understood by using the reaction coordinate diagrams in Figure 1. The upper part of the figure shows the relative energies of the three contributing configurations that describe the electronic structure of exciplexes as a function of the distance between the acceptor and donor (r_{A-D}). For conventional exciplex formation, the energy of the ($A^{\bullet-}D^{\bullet+}$) configuration rises when r_{A-D} is significantly less than van der Waals contact (dashed blue curve). In the formation of a bonded exciplex, the energy of this configuration decreases with decreasing r_{A-D} because of bond formation (solid blue curve). Thus, the energy of the charge-transfer configuration as a function of the donor−acceptor distance is the critical difference between conventional and bonded exciplexes.

Shown in the lower part of Figure 1 is a configuration mixing diagram—of the type pioneered by Shaik and co-workers[5]—for formation of a bonded exciplex. Mixing of the bonded ($A^{-}-D^{+}$) and the LE configurations (A*D) at large r_{A-D} leads to an avoided crossing that ultimately lowers the energetic barrier for reaction of A* + D via charge transfer. In the case of pyridine with the cyanoaromatic acceptors, the bonded configuration is sufficiently low in energy at smaller r_{A-D} that it results in another intended crossing with the ground configuration (green curve).[1] This a second avoided crossing causes the ground-state energy curve (lower black curve) to deviate from the purely repulsive behavior expected in the absence of configuration mixing. The deviation from repulsive behavior is observed in ground-state DFT computations for pyridine with several acceptors,[1] providing strong evidence for the mixing diagram in Figure 1. The crossing of the bonded and ground configurations also results in a small energy gap between the excited and the ground state, which accounts for the rapid excited-state deactivation observed in these reactions.

† Part of the "Sason S. Shaik Festschrift".
* Corresponding authors.
‡ University of Rochester.
§ Schrödinger, Inc.
|| Arizona State University.

10.1021/jp8041445 CCC: $40.75
Published on Web 10/24/2008

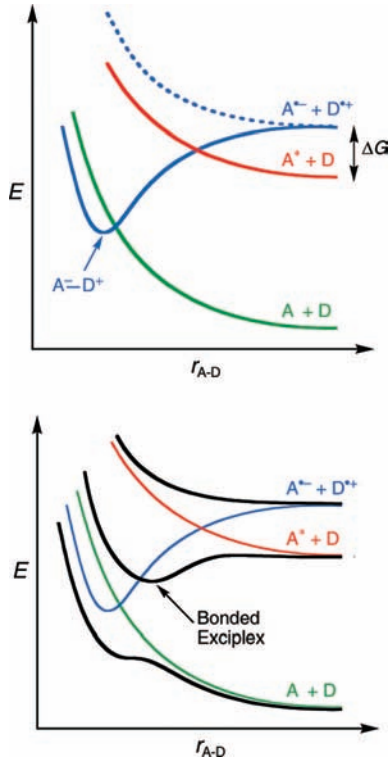

Figure 1. Schematic representation of energies of charge transfer (blue curves), LE (red curves,) and ground (green curves) configurations involved in bonded exciplex formation as a function of separation distance between the electron acceptor (A) and the electron donor (D), r_{A-D}. The charge-transfer configuration resembles a radical−ion pair at large separation distances ($A^{\bullet-}D^{\bullet+}$) and a bonded zwitterion ($A^{-}-D^{+}$) at short separation distances. The dashed blue curve represents the electron-transfer state when no bond is formed between $A^{\bullet-}$ and $D^{\bullet+}$.

This paper describes further experimental and computational studies on the quenching mechanism for reaction of pyridine and related donors with excited-state electron acceptors. Structure−reactivity relationships are explored for substituted pyridines. In addition, the importance of stereoelectronic effects is investigated by comparing quenching efficiencies in fluid solution versus solid solution. Finally, a new example of bonded exciplex formation is proposed for reaction of the singlet excited state of 2,6,9,10-tetracyanoanthracene with an ether as the donor.

Experimental Section

Materials. 9,10-Dicyanoanthracene, 1-cyanonaphthalene, and 2,6,9,10-tetracyanoanthracene were available from previous studies.[1] Pyridine derivatives were available from commercial sources and were purified by distillation or recrystallization before use. All solvents were HPLC grade and were used as received. Polystyrene, poly(4-methoxystyrene), and poly(vinylpyridine) were obtained from commercial sources and used as received. Poly(ethylene terephthalate) (Estar) film backing, which had a thin (<0.5 μm) latex layer (15/79/6 acrylonitrile/vinylidene chloride/acrylic acid) to improve coating adhesion, was a gift from Eastman Kodak.

Instrumentation. Fluorescence spectra were recorded on a spectrofluorometer equipped with double-grating excitation and emission monochromators, a 450 W xenon arc lamp source, and a thermoelectrically cooled photomultiplier tube detector. Spectra were continuously corrected for fluctuations in excitation intensity. Corrections for PMT response were applied to all spectra on the basis of calibration with a standard lamp according to the manufacturer's instructions.

TABLE 1: Rate Constants for Quenching of Singlet Excited 9,10-Dicyanoanthracene (DCA) and 1-Cyanonaphthalene (1CN) by Pyridine Derivatives in Argon-Purged Acetonitrile[a]

pyridine substituents	k_q (10^9 M^{-1} s^{-1}) DCA	k_q (10^9 M^{-1} s^{-1}) 1CN	relative energies of nonbonding orbitals
none	3.5	2.0	0.00
3-CN	0.27	(1.4)[b]	−0.73
4-CN	0.58	(6.7)[b]	−0.72
3-Me	4.0	2.6	+0.12
4-Me	4.0	2.4	+0.09
3-MeO	3.8	2.3	+0.07
4-MeO	4.0	2.4	+0.06
2-Me	2.1	1.4	
2-Et	1.5	0.85	
2,6-diMe	0.089	0.036	
2-MeO	~0.1[c]	0.15[c]	−0.27

[a] Relative energies (in eV) of the nonbonding orbitals of substituted pyridines versus pyridine calculated at the B3LYP/6-311+G** level of theory. [b] Quenching via electron transfer from 1CN* to the cyanopyridine (see text). [c] Some conventional exciplex emission observed (see text).

Preparation of Polymer Films. Dichloromethane solutions of the polymer and DCA (15 and 0.03% by weight, respectively) were knife-coated by using a 125 μm draw-bar coating knife on 100 μm thick Estar film backing. The Estar support was mounted on an aluminum coating block that was maintained at 23−25 °C by a circulating water bath. The coating block had a hinged cover that was closed to protect the coating while air drying. After drying on the coating block for 10−20 min, the coatings were further dried at 80 °C for 5 h giving ~15 μm thick films containing ~0.01 M DCA. Films were examined by UV−vis spectroscopy in multiple locations at the λ_{max} of DCA to test uniformity of the film thickness. The fluorescence spectra were recorded by excitation at isosbestic points between 370 and 430 nm.

Fluorometry. The rate constants for excited state quenching in solution were determined as described previously.[1]

Film samples with and without quencher were cut by using a 1.5″ arch punch and mounted between two 1.5″ diameter quartz disks in a Newport LH-150 mount. The mount was secured in a spectrofluorometer with a home-built stage. Spectra were recorded in front face mode, and samples were excited at isosbestic points between 370 and 430 nm. The emission spectrum of an identically mounted film of Estar support was used to background correct all emission spectra.

Computational Methods. Calculations were performed by using Jaguar v7.0 (release 109) (Schrödinger, Inc.: Portland, OR). Default settings were used throughout with the exception of the convergence criteria energy change, which was set to 10^{-6} Hartree. The solvent, dioxane, was defined in Jaguar by using the following parameters: dielectric constant = 2.21, FW = 88.1, and density = 1.034. The fraction of charge transfer was calculated from the atomic charges of the relevant moieties by using the NBO[6] option in Jaguar.

Results and Discussion

Rate Constants for Reaction of Substituted Pyridines. Rate constants for quenching of the singlet excited states of 9,10-dicyanoanthracene (DCA*) and 1-cyanonaphthalene (1CN*) by substituted pyridine derivatives were measured to investigate the nature of the substituent effects. We begin by discussing the quenching data for reaction of the 3- and 4-substituted pyridines with DCA*. As shown in Table 1, introduction of the electron-withdrawing cyano substituent at C3 or C4 leads

to a significant reduction of the rate constant for quenching of DCA* relative to pyridine. Interestingly, electron-donating substituents (Me and MeO) at C3 or C4 result in only a small rate enhancement. These results can be readily understood in terms of the bonded exciplex model.

As shown in Figure 1, the activation barrier for bonded-exciplex formation from diffusional encounter of A* and D depends upon the energy gap between the LE configuration (red curve) and the charge-transfer (CT) configuration (solid blue curve). Raising the energy of the CT configuration relative to the LE configuration results in a crossing of these configurations at a higher energy, leading to a larger activation barrier for bonded exciplex formation. For quenching of DCA* by pyridines, the energy gap at the A/D contact distance is determined by the reduction potential of DCA* and the pyridine oxidation potential that corresponds to removal of an electron from the nonbonding molecular orbital, that is, the orbital that is largely composed of the nonbonding pair of electrons on nitrogen. Because these oxidation potentials cannot be determined experimentally, the relative oxidation potentials were instead estimated from the nonbonding orbital energies. The energies of the pyridine nonbonding orbitals were computed by using the B3LYP hybrid density functional with a 6-311+G** basis set. This level of theory correctly predicts that the HOMO of pyridine is nonbonding in character.[7] The computations reveal that the relative electron energies in the nonbonding orbitals of the 3- and 4-CN substituted pyridines are significantly lower than that of pyridine (Table 1). By assuming these energies reflect the relative energies of the charge-transfer configurations, they predict that the 3- and 4-CN substituted pyridines should quench DCA* with smaller rate constants than that for pyridine, consistent with experiment. In contrast, the nonbonding orbital energies for the 3-Me-, 4-Me-, 3-MeO-, and 4-MeO-substituted pyridines are predicted to be only marginally higher than that of pyridine (Table 1), which explains why these pyridines quench DCA* with rate constants that are only slightly greater than that for pyridine (Table 1).

The addition of alkyl substituents at the ortho carbon(s) of pyridine leads to a reduction in the rate constant for quenching of DCA* (cf. 2-Me, 2-Et, and 2,6-Me_2 in Table 1). These results are consistent with steric effects previously reported.[1,8] Interestingly, introduction of a 2-MeO substituent leads to a surprisingly large decrease in the quenching rate constant for DCA* (Table 1). The effect is much larger than can be simply accounted for by the steric size of the methoxy substituent. For example, the steric *A* value[9] for a methoxy group (~0.6) is significantly less than even that for methyl (1.7); yet, k_q for 2-MeOPy is 22 times less than that for 2-MePy. MO calculations suggest that the smaller rate constant for 2-MeOPy has, in part, an electronic origin. The energy of the nonbonding orbital for 2-MeOPy is calculated to be ~0.3 eV lower than that for pyridine (Table 1). The electronic effect is insufficient to completely explain the slow quenching of 2-MeOPy, however. On the basis of orbital energies, 2-MeOPy is expected to be significantly more reactive than 3- and 4-CNPy, in disagreement with experiment. We suggest that the unusually low reactivity of 2-MeOPy can be explained by a specific steric effect. Previous work has shown that 2-MeOPy strongly prefers an *s-cis* conformation.[10] This conformation places the methyl group in the plane of the pyridine ring and syn to the nitrogen (see below), which increases the effective steric size of the 2-MeO substituent and explains the unusually low reactivity of 2-MeOPy.

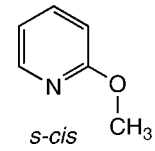

s-cis

We next turn to the quenching reactions with 1CN* (Table 1). The rate constants for quenching of 1CN* by 3-MePy, 4-MePy, 3-MeOPy, and 4-MeOPy parallel those for DCA* but are uniformly lower by a factor of ~1.6. Previous experiments have shown that the quenching rate constants for bonded-exciplex formation decrease as the reduction potential of the excited-state electron acceptor decreases.[1] Thus, the smaller quenching rate constants for 1CN* can be explained by its lower reduction potential versus DCA* (1.95 vs 1.99 V vs SCE, respectively).[1] Lower quenching rate constants versus DCA* are similarly observed for the quenching of 1CN* by 2-MePy, 2-EtPy, and 2,6-Me_2Py (Table 1), consistent with a steric effect on quenching. Surprisingly, 3-CNPy, 4-CNPy, and 2-MeOPy quench 1CN* more rapidly than DCA*. We propose that the increased reactivities with 1CN* in these cases are due to changes in the quenching mechanisms.

The greater reactivity of 1CN* with 3-CNPy and 4-CNPy can be explained by intervention of an electron transfer process involving electron transfer from 1CN* to 3-CNPy and 4-CNPy (eq 3). The energetics for this electron-transfer reaction are given by eq 4, where E_{D^*} and E_D^{ox} are the excited-state energy and the oxidation potential of the electron donor and E_A^{red} is the reduction potential of the acceptor. For 1CN, E_{D^*} and E_D^{ox} are 3.83 eV and 2.01 V vs SCE, respectively.[1,11] The reduction potentials for 3-CNPy and 4-CNPy are −2.00 and −1.80 V versus SCE, respectively.[12] Thus, the driving forces for electron transfer from 1CN* to 3-CNPy and 4-CNPy are energetically feasible in both cases. The contrasting behavior of 1CN* and DCA* in their reactions with 3-CNPy and 4-CNPy can be readily understood from the relative redox properties of the excited states. The E_{D^*} (2.90 eV)[1] and E_D^{ox} (1.75 V vs SCE)[13] values for DCA show that DCA* is a much poorer reducing agent than 1CN*. Thus, electron transfers from DCA* to 3-CNPy and 4-CNPy are highly endothermic (0.65−0.85 eV) and, consequently, expected to be too slow to play a role.

$$1CN^* + NC\text{-}Py \rightarrow 1CN^{\bullet+} + NC\text{-}Py^{\bullet-} \quad (3)$$

$$-\Delta G = E_{D^*} - (E_D^{ox} - E_A^{red}) \quad (4)$$

Finally, we discuss a unique aspect of the quenching reactions involving 2-MeOPy. Unlike all of the other pyridine quenching reactions, the quenching of both 1CN* and DCA* by 2-MeOPy results in partial formation of emissive exciplexes. These observations are consistent with competitive formation of bonded exciplexes and conventional exciplexes. Exciplex emission is relatively insignificant for DCA* but is substantial for 1CN* (Figure 2). The additional quenching mechanism for reaction of 1CN* with 2-MeOPy rationalizes the unexpected high rate constant for this reaction versus DCA*. Quenching by both conventional and bonded-exciplex formation for 2-MeOPy means that its quenching rate constants in Table 1 are the cumulative result of both processes.

Quenching Reactions in Polymeric Media. One of the ways that excited-state quenching via conventional exciplex formation should differ from bonded exciplex formation is that the latter reaction should have significantly more restrictive stereoelectronic requirements. For bonded-exciplex formation in fluid media, the specific orientation of the reactants required for bond

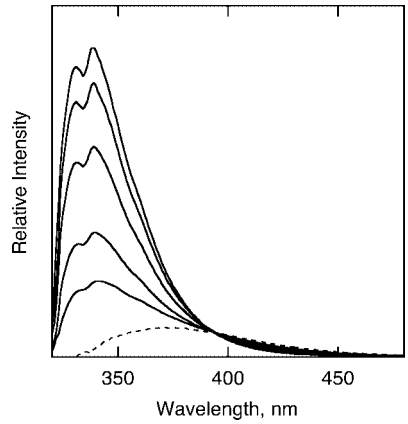

Figure 2. Emission spectra of 1CN* in acetonitrile in the presence of 2-methoxypyridine (0.0, 0.095, 0.285, 0.95, and 2.85 M, with decreasing intensity) and the extrapolated exciplex emission (dashed curve).

formation can be achieved during collisions in the encounter pair. If molecular rotation is restricted by the medium, however, bond formation should be limited to the subset of the reactants that can achieve the required orientation and separation distance during the excited-state lifetime. We sought to test this prediction by comparing excited-state quenching of conventional and bonded exciplexes in polymeric media.

Initially, quenching by conventional exciplex formation in polymers was tested by comparing the fluorescence of DCA* in a solid film of polystyrene (PS) versus in poly(*p*-methoxy)-styrene (PMeOS). The emission of DCA* is not quenched in toluene; therefore, no fluorescence quenching is expected in PS. Strong quenching is expected in PMeOS, however, because of the much lower oxidation potential of the polymer.[14] These expectations are indeed borne out by experiment. As shown in Figure 3A, the fluorescence of DCA* is >90% quenched in PMeOS relative to PS. In addition to a small amount of residual DCA* fluorescence, a weak, broad emission centered at ~515 nm is also observed in PMeOS, which we assign to conventional exciplex emission [see lower panel of Figure 3A]. Correcting for the exciplex emission by comparing spectrum b, instead of a, to the emission in PS, the quenching of DCA* in PMeOS is calculated to be 93.6%.

Fluorescence spectra were next measured for DCA* in films of PS versus poly(vinylpyridine), PVP, [see Figure 3B]. A quantitative analysis shows that the fluorescence of DCA* in PVP is quenched by only 34% in comparison with PS.

It is instructive to compare the quenching results in solid solution to those in fluid solution. As reported earlier, nearly complete quenching of DCA* emission is observed in pyridine.[1] For example, the ratio of the fluorescence quantum yields (Φ_f) for DCA* in pyridine versus in toluene, $(\Phi_f)_{pyridine}/(\Phi_f)_{toluene}$, is <0.01. In contrast, the corresponding ratio in the polymer films, $(\Phi_f)_{PVP}/(\Phi_f)_{PS}$, is 0.66. Thus, despite the high local concentration of pyridine moieties in PVP, relatively little quenching of DCA* occurs. These data are consistent with the prediction of the bonded exciplex model that a particular orientation of DCA* and pyridine must be possible for quenching to occur.

The quenching of DCA* in PVP can be further analyzed quantitatively. We begin by assuming that each DCA molecule in PVP is surrounded, on average, by a number of pyridine moieties (n) that can potentially quench the excited state. If the probability that a DCA* molecule is not quenched by an adjacent pyridine moiety is α, the probability that a DCA* molecule is not quenched by any of the nearest-neighbor

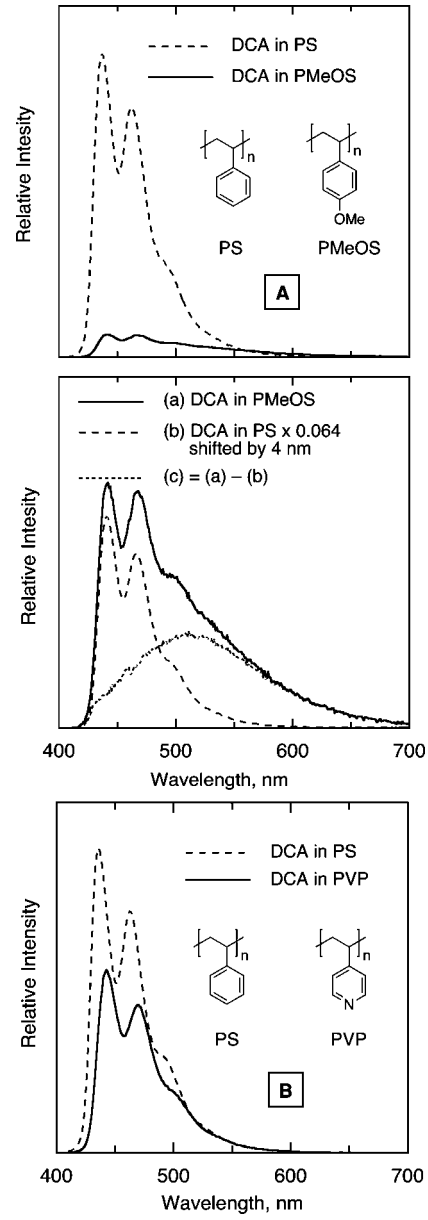

Figure 3. (A) Fluorescence spectra for 9,10-dicyanoanthracene in thin films of polystyrene (dashed lines) and poly(*p*-methoxystyrene) (solid line). (B) Fluorescence spectra for 9,10-dicyanoanthracene in thin films of polystyrene (dashed lines) and poly(vinylpyridine) (solid line).

pyridine moieties is α^n. A reasonable estimate for n in PVP is ~5.[15] Thus, for 66% of the DCA* molecules to be unquenched in PVP, an α of 0.92 is required; that is, only ~8% of the surrounding pyridine moieties are capable of quenching DCA*. This analysis illustrates the geometrically restrictive nature of the DCA*-pyridine quenching process. By comparison, α for DCA* in PMeOS is 0.58; that is, 42% of the surrounding anisyl moieties lead to exciplex formation. The 5-fold increase in quenching efficiency illustrates the geometrically restrictive nature of the bond-forming DCA*−pyridine quenching process, compared with the less restrictive $\pi-\pi$ overlap required for conventional exciplex formation.

Role of Bonded-Exciplex Formation in Radiationless Decay. Previous examples of bonded exciplexes have involved a variety of electron-deficient excited-state acceptors with pyridine donors. In prior work, we showed that reaction of the excited states of 2,6,9,10-tetracyanoanthracene (TCA) and 1,4-dicyanonaphthalene (DCN) with dioxane and 1,2-dimethoxy-

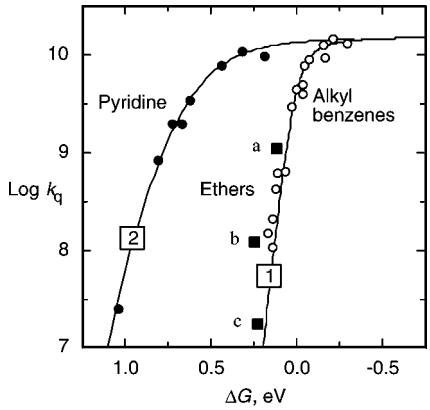

Figure 4. Logarithm of the rate constants for quenching of singlet excited-state cyanoaromatic acceptors by alkylbenzene donors (1, unfilled circles) and pyridine (2, filled circles) in acetonitrile vs the free energy (ΔG) of electron transfer from the donors to the excited-state acceptors. The filled squares are data for quenching of excited-state cyanoaromatic acceptors by dioxane and 1,2-dimethoxyethane as donors (see text).

TABLE 2: Deactivation Rate Constants of Singlet-Excited DCA and TCA in Different Solvents

acceptor	solvent	$\Sigma k = 1/\tau$ 10^6 s^{-1}	k_f 10^6 s^{-1}	k_{isc} 10^6 s^{-1}	k_{nr} 10^6 s^{-1}
TCA	trichloroethylene	84.7	66.1	6.8	11.9
TCA	dioxane	144.3	57.7	3.0	83.6
TCA	fluorobenzene	63.7	55.7	1.3	6.7
TCA	acetonitrile	59.5	53.6	*a*	<4.1
DCA	cyclohexane	87.0	79.6	1.0	6.3
DCA	carbon tetrachloride	88.5	81.4	1.1	6.0
DCA	trichloroethylene	89.3	80.4	2.1	6.9
DCA	dioxane	78.1	72.2	0.9	5.0
DCA	fluorobenzene	81.3	73.7	1.1	6.5
DCA	toluene	75.2	68.4	0.5	6.3
DCA	*p*-xylene	65.4	58.8	0.5	6.1
DCA	acetonitrile	67.1	59.1	*a*	<8.0

[a] not measured.

ethane (DME) in acetonitrile had quenching rate constants that were close to those expected for conventional electron transfer/exciplex formation [data points a−c in Figure 4).[16] We wondered whether similar quenching reactions in a nonpolar medium would slow the rate for conventional electron transfer/exciplex quenching sufficiently to permit bonded-exciplex formation to compete. Of the three quenching reactions previously studied, TCA/dioxane [data point a in Figure 4] was the most attractive to examine further, because the other two reactions already have relatively low quenching rate constants in acetonitrile, and decreasing the rate constants significantly further would likely result in other excited-state decay processes becoming dominant (e.g., monomer fluorescence).

Interestingly, the rate constant for decay of TCA* in neat dioxane was found to be significantly greater than that measured in several other solvents of widely varying polarity (Table 2).[17] The rate constants for decay of TCA* in these other solvents are quite similar to those of DCA*, which have been measured in an even wider range of solvents (Table 2). From measurements of the lifetimes of the excited states and the quantum yields for fluorescence and intersystem crossing, individual rate constants for fluorescence (k_f), intersystem crossing (k_{isc}), and nonradiative (k_{nr}) decay could be obtained by using eqs 5−7, as described previously.[17] The fluorescence yields were obtained by conventional steady-state fluorimetry,[17a] and the triplet yields were determined by a combination of transient absorption spectroscopy and time-resolved photoacoustic calorimetry.[17b]

$$k_f = \Phi_f/\tau_{Ex} \quad (5)$$

$$k_{isc} = \Phi_{isc}/\tau_{Ex} \quad (6)$$

$$k_{nr} = (1 - \Phi_f - \Phi_{isc})/\tau_{Ex} \quad (7)$$

This analysis revealed that k_f for both TCA* and DCA* fall within a narrow range in all of the solvents, $\sim 6-8 \times 10^7$ s^{-1}. In contrast, k_{nr} for TCA* in dioxane is roughly an order of magnitude larger than the other k_{nr} values ($\sim 84 \times 10^6$ s^{-1} vs $\sim 5-12 \times 10^6$ s^{-1}). Clearly, an additional deactivation path is responsible for most (>90%) of the nonradiative decay of TCA* in dioxane.

It is easy to demonstrate that the unusually large k_{nr} for TCA* in dioxane is not due to conventional exciplex formation. The rate constant for conventional exciplex formation between TCA and dioxane can be estimated from the quenching rate constant for reaction of TCA* with toluene in dioxane. TCA* reacts with toluene in dioxane by conventional exciplex formation with a quenching rate constant (k_q) of 1.5×10^8 M^{-1} s^{-1} (see Supporting Information). This rate constant can be used to determine the unimolecular rate constant for in-cage exciplex formation between TCA* and toluene (k_{ex}) by using eq 8, where k_d and k_{-d} are the diffusion rate constants for formation and separation, respectively, of the TCA*/toluene contact pair. The diffusional encounter rate constant (k_d) in dioxane at 20 °C was calculated from the Smoluchowski equation[18] to be 5.4×10^9 M^{-1} s^{-1}. The separation rate constant (k_{-d}) was calculated to be 9.9×10^9 s^{-1} from the Eigen equation.[19] These values lead to a rate constant for exciplex formation (k_{ex}) of 2.8×10^8 s^{-1}. We have previously reported that the oxidation potential for dioxane is ~0.22 V greater than that for toluene.[1] Given that electron transfer in the endergonic region falls off by an order of magnitude for each ~0.06 eV decrease in driving force,[4,20] k_{ex} for TCA*/toluene can be used to predict k_{ex} for TCA*/dioxane. This leads to $k_{ex} \approx 6 \times 10^4$ s^{-1} for TCA*/dioxane, which is about three orders of magnitude less than the measured k_{nr} for TCA* in dioxane. Thus, conventional exciplex formation clearly cannot explain the high nonradiative decay rate constant for TCA* in dioxane. Instead, we propose that bonded-exciplex formation can. Indirect support for the bonded exciplex hypothesis was obtained from quantum chemical calculations, as described below.

$$k_q = \frac{k_d\, k_{ex}}{k_{-d} + k_{ex}} \quad (8)$$

The configuration mixing model shown in Figure 1 predicts that interaction of the bonded charge-transfer configuration with the repulsive ground configuration will lead to a significant lowering of the ground-state energy and that the interaction will increase with decreasing bond distance between the acceptor and the donor. In general, the lower the energy of the charge transfer configuration, the lower the energy of the ground state will be. Shown in Figure 5 are the energy profiles for addition of dioxane to TCA and DCA as a function of r_{C-O} interatomic distance. The B3LYP hybrid-functional method was used for the calculations with a 6-31+G** basis set and a self-consistent reaction field (SCRF) model to simulate the solvent, dioxane. All calculations were corrected for basis set superposition error by using the counterpoise method[21] and geometries were fully optimized at each r_{C-O} distance. Addition to C1 of TCA and C2 of DCA were found to give the lowest energy structures.

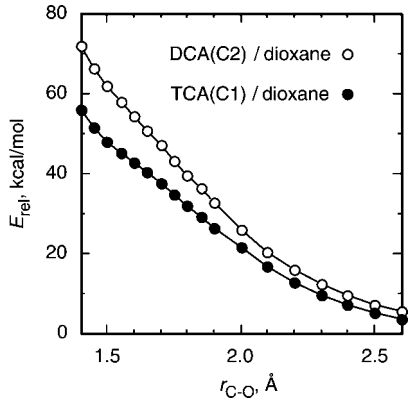

Figure 5. Computed ground-state energies as a function of interatomic distance, r_{C-O}, for ground-state addition of dioxane to C2 of DCA (unfilled circles) and C1 of TCA (filled circles). The computations were performed by using the B3LYP hybrid functional method with a 6-31+G** basis set, counterpoise corrected, and in a dielectric continuum corresponding to dioxane. $E_{rel} = 0$ at $r_{C-O} = \infty$.

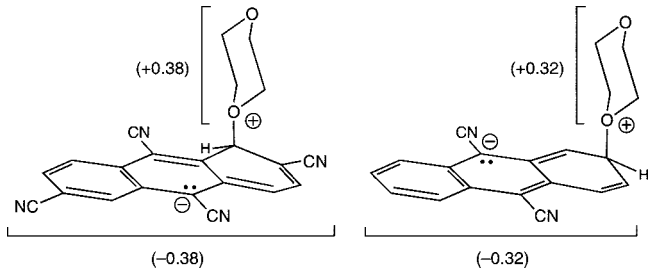

Figure 6. Computed ground-state structures (B3LYP/6-31+G**) and natural bond order (NBO) fragment charges for addition of dioxane to TCA and DCA at $r_{C-O} = 1.6$ Å.

The calculations reveal that the ground-state energy for TCA/dioxane is uniformly lower than that for DCA/dioxane and that the energy difference increases with decreasing r_{C-O} distance. It is also noteworthy that the TCA/dioxane profile shows a weak inflection point at $r_{C-O} \approx 1.7$ Å. As previously discussed, an inflection point in the ground-state energy profile for addition of pyridine to various acceptors is evidence for the existence of a low-lying bonded charge-transfer configuration.[1] Although the inflection point is less well defined in the case of TCA/dioxane, the lower energy of the potential energy surface relative to that of DCA/dioxane suggests that the energy gap between the ground and bonded configurations is smaller for TCA than for DCA. This should result in a greater extent of configuration mixing for TCA/dioxane, which, in turn, should lead to a larger extent of charge-transfer character in the ground state. The computed fragment charges TCA/dioxane and DCA/dioxane are consistent with this prediction (Figure 6).

The calculated energies and fragment charges are both consistent with the charge transfer configuration for TCA/dioxane having a deeper energy minimum than for DCA/dioxane. Thus, as the r_{C-O} distance decreases beyond van der Waals contact, the energy of the TCA/dioxane bonded configuration will decrease more rapidly, leading to a greater mixing with the TCA*/dioxane LE configuration (cf. Figure 1). This will result in a lower reaction barrier for bonded-exciplex formation. It is worth noting that the present data do not exclude the possibility that a bonded exciplex could also exist for DCA/dioxane; however, the experimental quenching data show that the activation barrier for bonded-exciplex formation is too high to compete with the normal excited-state decay processes in this case. In contrast, the lower barrier for bonded-exciplex formation with TCA/dioxane provides a new reaction channel for excited-state decay, which manifests itself as an unusually large rate constant for nonradiative decay. This should be a general experimental feature for bonded-exciplex formation.

Conclusions

The experiments discussed here expand and provide additional support for the bonded-exciplex model that we recently proposed to explain the quenching reactions of excited electron acceptors with pyridine. For example, the electronic effect of substituents at the 3- and 4- positions of pyridine on the quenching rate constants correlate with the energy of the nonbonding, pyridine molecular orbital, consistent with the expectations of a qualitative configuration mixing model for bonded-exciplex formation. Examples of the delicate balance between the formation of conventional exciplexes and/or bonded exciplexes are also presented. This balance is further illustrated by a change in mechanism that explains seemingly contradictory results for the quenching of two cyanoaromatics by cyanopyridines, where one reaction proceeds via bonded exciplex-formation and the other by electron transfer from the cyanoaromatic excited state to the cyanopyridines. Additional support for the bonded-exciplex mechanism is provided by comparing reactions in fluid media with those in poly(vinylpyridine), where the restrictive environment of the polymer inhibits attainment of the proper orientation for bond formation. Finally, the formation of bonded exciplexes is expanded to donors beyond pyridines to include ethers, which suggests a broader scope to the bonded-exciplex model.

Acknowledgment. Research support was provided by the National Science Foundation (CHE-0749919) and the Research Corporation. We thank Paul B. Merkel (University of Rochester) for determining the reduction potential of 4-cyanopyridine. We are grateful to Prof. Sason Shaik (Hebrew University) for stimulating discussions during the course of this work.

Supporting Information Available: Fluoresence spectra of 2,6,9,10-tetracyanoanthracene (TCA) in dioxane and TCA + 0.5 M toluene in dioxane. This information is available free of charge via the Internet at http://pubs.acs.org.

References and Notes

(1) Wang, Y.; Haze, O.; Dinnocenzo, J. P.; Farid, S.; Farid, R.; Gould, I. R. *J. Org. Chem.* **2007**, *72*, 6970.

(2) Weller, A. *Z. Phys. Chem. (Munich)* **1982**, *130*, 129.

(3) Because of the large energy gap between the ground configuration and both the LE and radical−ion pair configurations, the contribution from the ground configuration (c_3, eq 1) to the exciplex state is usually negligible.

(4) Rehm, D.; Weller, A. *Isr. J. Chem.* **1970**, *8*, 259.

(5) (a) Shaik, S. S. *J. Am. Chem. Soc.* **1981**, *103*, 3692. (b) Pross, A.; Shaik, S. S. *Acc. Chem. Res.* **1983**, *16*, 363. (c) Shaik, S. S. *Prog. Phys. Org. Chem.* **1985**, *15*, 197. (d) Shaik, S. S. In *New Theoretical Concepts for Understanding Organic Reactions*; Bertrán, J., Csizmadia, I. G., Eds.; NATO ASI Series; Kluwer: Dordrecht, 1989; Vol. C267, p 165. (e) Shaik, S.; Shurki, A. *Angew. Chem., Int. Ed.* **1999**, *38*, 586. (f) Shaik, S. S.; Hiberty, P. C. *A Chemist's Guide to Valence Bond Theory*; Wiley: New York, 2008.

(6) Glendening, E. D.; Badenhoop, J, K.; Reed, A. E.; Carpenter, J. E.; Bohmann, J. A.; Morales, C. M.; Weinhold, F. *NBO 5.0.*; Theoretical Chemistry Institute: University of Wisconsin, Madison, 2001.

(7) For a literature summary regarding the assignment of the lowest ionic state of pyridine, see: Tsubouchi, M.; Suzuki, T. *J. Phys. Chem. A* **2003**, *107*, 10897.

(8) (a) Jacques, P.; Burget, D. *J. Photochem. Photobiol. A* **1992**, *68*, 165. (b) Jacques, P.; Allonas, X. *J. Photochem. Photobiol. A: Chem.* **1994**, *78*, 1.

(9) Eliel, E. L.; Wilen, S. H.; Mander, L. N. *Stereochemistry of Organic Compounds*; Wiley: New York, 1994; pp 695−700.

(10) (a) Lumbroso, H.; Bertin, D. M. *Bull. Soc. Chim. Fr.* **1970**, *1728*. (b) Favini, G.; Raimondi, M.; Gandolfo, C. *Spectrochim. Acta* **1968**, *24A*, 207. (c) Contreras, R. H.; Facelli, J. C.; de Kowalewski, D. G. *Org. Magn. Reson.* **1982**, *20*, 40. (d) Blonski, W. J. P.; Hruska, F. E.; Wildman, T. A. *Org. Magn. Reson.* **1984**, *22*, 505. (e) Contreras, R. H.; Beikofsky, R. R.; de Kowalewski, D. G.; Orendt, A. M.; Facelli, J. C. *J. Phys. Chem.* **1993**, *97*, 91.

(11) Schmidt, R.; Shafii, F.; Schweitzer, C.; Abdel-Shafi, A. A.; Wilkinson, F. *J. Phys. Chem. A* **2001**, *105*, 1811.

(12) The reduction potential of 4-CNPy was determined vs 1-cyanonaphthalene by redox equilibration by using a method analogous to that previously described; Guirado, G.; Fleming, C. N.; Lingenfelter, T. G.; Williams, M. L.; Zuilhof, H.; Dinnocenzo, J. P. *J. Am. Chem. Soc.* **2004**, *126*, 14086. (b) The reduction potential of 3-CNPy was determined from the value for 4-CNPy and the difference in eletrochemical reduction potentials reported previously; Loutfy, R. O.; Loutfy, R. O. *Can. J. Chem.* **1973**, *51*, 1169)

(13) Based on the reported difference in oxidation between DCA and 9,10-diphenylanthracene (DPA) of 0.57 V (a) Clegg, A. D.; Rees, N. V.; Klymenko, O. V.; Coles, B. A; Compton, R. G. *J. Am. Chem. Soc.* **2004**, *126*, 6185 and the oxidation potential reported for DPA of 1.18 V vs SCE in acetonitrile (b) Sioda, R. E. *J. Phys. Chem.* **1968**, *72*, 2322.

(14) The difference in oxidation potential for PS and PMeOS can be roughly approximated by the difference in the oxidation potentials of toluene and 4-methylanisole, which are 2.33 and 1.53 V vs SCE, respectively (ref 1 and. Suzuki, T.; Fujii, H.; Yamashita, Y.; Kabuto, C.; Tanaka, S.; Harasawa, M.; Mukai, T.; Miyashi, T. *J. Am. Chem. Soc.* **1992**, *114*, 3034)

(15) Farid, S.; Daly, R. C.; Moody, R. E.; Huang, W.-Y.; Reiser, A. *Macromolecules* **1991**, *24*, 4041.

(16) Adapted with permission from ref 1. Copyright 2007 American Chemical Society.

(17) (a) Gould, I. R.; Young, R. H.; Mueller, L. J.; Farid, S. *J. Am. Chem. Soc.* **1994**, *116*, 8176. (b) Gould, I. R.; Farid, S. *J. Phys. Chem. B* **2007**, *111*, 6782.

(18) (a) Smoluchowski, M. V. *Phys. Z.* **1916**, *17*, 557. (b) Smoluchowski, M. V. *Phys. Z.* **1916**, *17*, 583. (c) k_d was calculated from the Smoluchowski equation ($k_d = 4\pi N r_{A+D} D_{A+D}/1000$) with $r_{A+D} = 6$ Å and $D_{A+D} = 1.2 \times 10^{-5}$ cm^2 s^{-1}, where the diffusion coefficient D_{A+D} is calculated from the Stokes-Einstein equation ($D_{A+D} = D_A + D_D = RT/6\pi\,\eta r_A N + RT/6\pi\,\eta r_D N$) with $\eta = 1.2$ cP, $T = 293$ K, and $r_A = r_D = 3$ Å.

(19) (a) Eigen, M. Z. *Phys. Chem.* **1954**, *1*, 176. (b) $k_{-d} = 3000\ k_d/4\pi (r_{A+D})^3\ N = 9.9 \times 10^9$ s^{-1} if $k_d = 5.4 \times 10^9$ M^{-1} s^{-1} and $r_{A+D} = 6$ Å.

(20) Cf. line 1 in Figure 4 for $\Delta G > 0$.

(21) Ratner, M. A.; Schatz, G. C. *Introduction to Quantum Mechanics in Chemistry*; Prentice Hall: Upper Saddle River, NJ, 2001; p 230.

JP8041445